

# A new high-resolution method for measuring cosmic ray composition beyond 10 TeV

S. P. Wakely<sup>1</sup>, D. B. Kieda<sup>2</sup>, and S. P. Swordy<sup>3</sup>

<sup>1</sup>Enrico Fermi Institute, University of Chicago, Chicago, IL 60637, U.S.A.

<sup>2</sup>Department of Physics, University of Utah, Salt Lake City, UT 84112, U.S.A.

<sup>3</sup>Enrico Fermi Institute, Department of Physics, and Department of Astronomy and Astrophysics, University of Chicago, Chicago, IL 60637, U.S.A.

**Abstract.** A new high-resolution method for the determination of cosmic ray elemental composition beyond 10 TeV is presented. The technique combines a measurement of the Čerenkov light produced by the incoming cosmic-ray nucleus in the upper atmosphere with an estimate of the total nucleus energy produced by the extensive air shower initiated when the particle interacts deeper in the atmosphere. The emission regions prior to and after the first hadronic interaction can be separated by an imaging Čerenkov system with sufficient angular and temporal resolution. The expected charge resolution of the technique is  $\Delta Z/Z < 5\%$  for incident iron nuclei in the region of the “knee” of the cosmic-ray energy spectrum. This resolution is essentially independent of hadronic interaction model.

---

## 1 Introduction

In this paper we describe an new idea (Kieda, Swordy, and Wakely, 2000) which may allow high-resolution cosmic ray composition measurements at the knee to be made from the ground. This idea has become possible through advances in the imaging atmospheric Čerenkov technique and is based on the conjecture that a detector of fine-enough pixelation will be capable of observing Čerenkov light emitted directly from cosmic ray nuclei prior to their first interaction in the atmosphere. Under most circumstances, this light is overwhelmed by the Čerenkov emission from the subsequent extensive air shower (EAS). However, with an appropriate detector, and within certain geometric constraints, this “direct Čerenkov”, or DČ, light can be sufficiently well separated from the background of EAS Čerenkov light to make high-precision measurements of the cosmic ray composition in the energy region of the knee. In an accompanying paper in this conference, we discuss the observational implications of the technique (Kieda, Swordy, and Wakely, 2001).

---

*Correspondence to:* S.P. Wakely (wakely@uchicago.edu)

## 2 Method

Methods targeting DČ light are not entirely new. In 1965, Sitte proposed that this radiation might be observed in high-altitude balloon-borne instruments. His idea, which was revisited by Gough (1976), was to place detectors at a height in the atmosphere above the mean interaction point of heavy primary cosmic rays and to look for the direct production of Čerenkov light. In the absence of the large EAS Čerenkov background, it was expected that direct Čerenkov yields would provide accurate composition measurements. After a pioneering flight by Sood (1983), the concept was unexploited until recent efforts by Clem, *et al.* (2001). With the current ground-based technique the fundamental challenge is the identification of the DČ light against the background EAS Čerenkov light which the balloon-borne instruments avoid.

### 2.1 Čerenkov Radiation

The current technique relies on two important features of Čerenkov radiation. The first feature is that (assuming a fixed particle energy) the Čerenkov yield depends only on the charge of the particle (as  $Z^2$ ), and the local density of the atmosphere surrounding that particle. Therefore, when the density is known, a measurement of the Čerenkov yield provides a strong estimation of the particle mass.

The second important feature of Čerenkov radiation is that the local atmospheric density *entirely* determines the geometry of emission. This is important because the atmospheric density itself is a function of the height in the atmosphere. Therefore, the pattern of Čerenkov emission is uniquely defined by an atmospheric density profile. This can be seen in the upper panel of Figure 1, which shows the impact parameter (*i.e.*, radius from the shower trajectory) of Čerenkov photons as a function of their emission heights. From the figure, it can be seen that for a given particle trajectory, Čerenkov photons can be matched by their emission angle and impact parameter to unique emission heights in the atmosphere. Therefore, DČ light emitted by a primary particle high in the

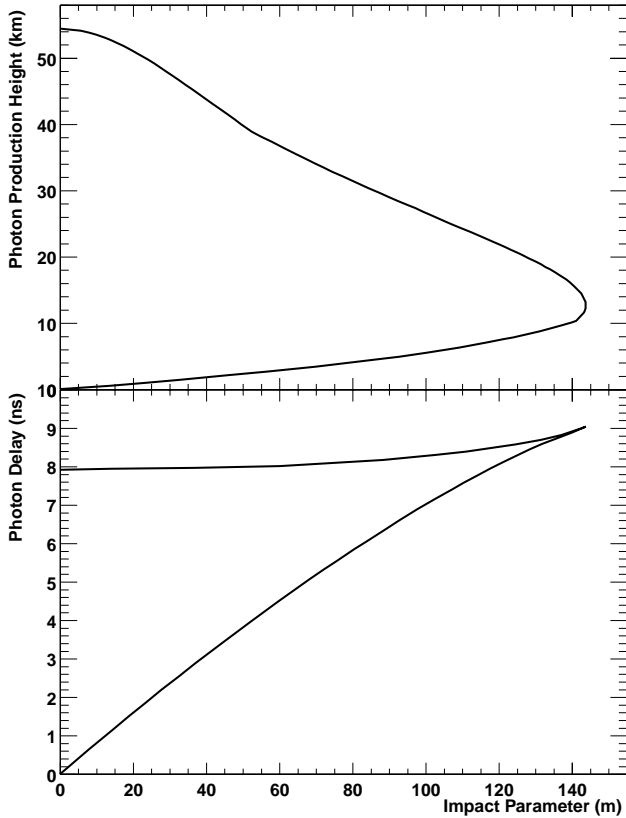


**Fig. 1.** The direct Čerenkov emission characteristics of a single non-interacting particle vertically incident on the atmosphere. Upper Panel: The impact parameter of photons at sea level relative to the original particle trajectory versus the emission height. Lower Panel: The photon time delay at sea level relative to the particle traveling at speed  $c$  versus the emission height. The default CORSIKA atmospheric profile is used.

atmosphere may be differentiated from Čerenkov light emitted from EAS particles lower in the atmosphere. Once these photons are separated from the EAS background and correlated to an emission height, the local density can be determined, and the total DČ yield used to estimate the particle charge.

The geometry of the DČ emission leads to a very fast time structure at high altitude. All of the photons emitted from altitudes higher than 30 km arrive within roughly 300 ps of each other. Furthermore, this light is delayed with respect to the light emitted lower in the atmosphere (*e.g.*, below 5 km) by 3 ns or more, depending on the observation radius. This leads to an additional method for differentiating between the DČ light and that produced in the EAS. The DČ should be delayed from the main Čerenkov pulse, and should have a characteristic width over an order of magnitude shorter than the  $\sim 6$  ns EAS Čerenkov pulse. The photon arrival times (measured w.r.t a particle moving at  $c$ ) are shown in the bottom panel of Figure 1.

Since the rate of emission of Čerenkov light increases with atmospheric depth (because the density becomes larger), the DČ yield will improve with increasing impact parameter (up

to  $R \approx 145$  m). However, since most nuclei interact by altitudes of 25 km or so, the best impact parameter must be chosen as a compromise between high DČ density (low altitude), and low interaction probability (high altitude). A reasonable radius is  $\sim 80$  m. At this distance, the angular scale of DČ light will be at  $\sim 0.15^\circ$ , compared to the EAS angular scale of  $\gtrsim 0.20^\circ$ .

The choice of observation radius also has an impact on the timing separation between the DČ light and the majority of the EAS light. For this purpose,  $\sim 80$  m is again good compromise between providing an adequate DČ signal before the particle is likely to interact and maintaining some time separation between the DČ and EAS signal.

## 2.2 Average Behavior

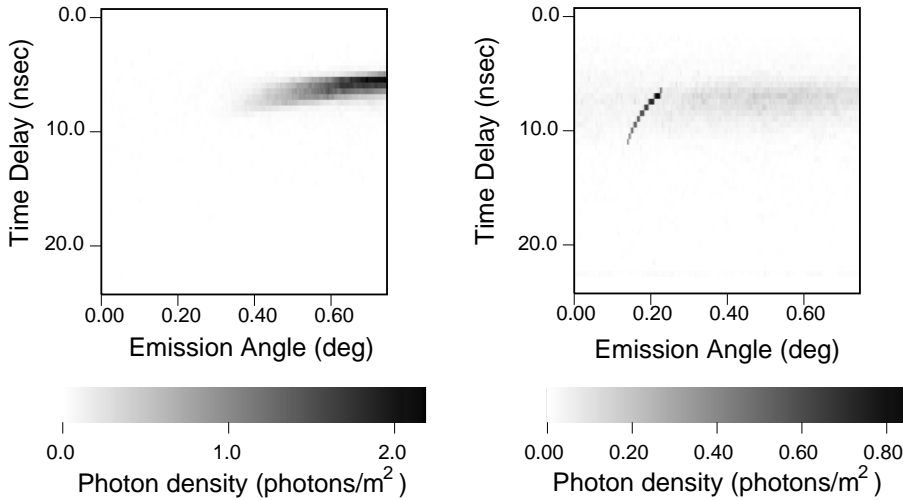
We have modeled the behavior of EAS including DČ light using a modified MOCCA Monte Carlo Simulation (Hillas, 1982a,b; Kieda, 1995) and also the CORSIKA (Version 5.945, QGSJet98) simulation package (Heck, 1998). Both of these codes yield similar results, and predict that DČ light should be observable against the background EAS Čerenkov light over an energy window which depends on the charge of the primary particle.

Figure 2 illustrates the basis of the DČ technique by showing the light collected in time/angle bins from two vertical particles. The left panel shows a 10 TeV gamma ray, and the right panel shows a 10 TeV  $Z = 12$  (Mg) nucleus. In the plot for Mg, the DČ light emission is clearly seen as a high-density arc on the left of the figure, separated from the Čerenkov emission produced by the EAS (which appears as a blob to the right). Additional details of the simulation are contained in the caption for the figure.

Our studies have shown that the DČ technique is effective over a limited range of particle energies. The lower energy limit is defined by the threshold for Čerenkov emission, while the upper energy limit is set by background light production in the EAS. At some energy, the photon densities due to EAS Čerenkov light will approach and exceed those of the direct light. When that occurs, the DČ ‘arc’ in the time-angle plot will no longer be observable against the background. The resulting energy window scales with the charge of the primary particle as  $\sim Z$  for heavy nuclei. This result, which has been verified by simulations, arises essentially because the DČ light scales like  $Z^2$ , whereas the background level scales like  $Z$ . For Iron nuclei, the measurement window spans between roughly 20 TeV and 1000 TeV.

## 3 Background and Resolution Considerations

We have examined, via Monte Carlo simulations, the impact of various background effects on the resolution of the DČ technique. In general, these effects can be divided into three groups: background light and scattering effects, detector resolution effects, and hadronic interaction effects. We describe each of these and their  $Z$  dependence, and present a compos-



**Fig. 2.** Simulated DČ and EAS Čerenkov light emitted from vertically incident particles. The left panel shows a 10 TeV gamma ray, and the right panel a 10 TeV  $Z = 12$  (Mg) nucleus. The light is collected in an annulus 67 – 94 m (mean radius 80 m) about the shower axis. The vertical axis is the time delay of arriving photons with respect to a vertical particle traveling at  $c$ . The horizontal axis is the arrival angle of the photons with respect to the vertical at the observing site. The Čerenkov light has been integrated over the wavelength band of 300 – 600 nm. The scales below each panel indicate the photon densities.

ite plot of the predicted charge resolution as a function of the primary charge  $Z$ .

### 3.1 Background Light and Scattering Effects

Background light sources which may degrade the charge resolution of this technique include fluctuations in the night sky background level, fluctuations in the secondary Čerenkov light emitted by the extensive air shower, and secondary light which is scattered by the atmosphere into the same time-angle bins as the DČ light signal.

The overall background expected by fluctuations in the night-sky light level can be determined from previous measurements at dark sites. The standard background value quoted is  $2 \times 10^{12}$  photons/(m<sup>2</sup> sec sr) over the range 300 – 600 nm. This translates to an overall rms intensity scale near 0.01 photons/m<sup>2</sup> for the angle/time bin sizes used in Figure 2, substantially smaller than the typical DČ signal. This quantity is independent of the primary charge  $Z$ . Since the DČ signal increases as  $Z^2$ , the night sky background contribution to the charge resolution  $\Delta Z/Z$  decreases like  $1/Z^2$ .

The second, and most prominent, background source is Čerenkov light emitted from the EAS electrons themselves. Since the threshold energy for observing DČ light increases linearly with increasing  $Z$ , the secondary Čerenkov light background, which is proportional to primary energy, also increases linearly. In principle, since the primary cosmic ray energy is measured from the secondary Čerenkov light, the amount of secondary background light in the DČ pixel bins could be estimated. This could be subtracted out to yield a pure DČ light measurement. However, Poisson variations in the secondary Čerenkov background will generate fluctuations in the background-subtracted signal, thereby limiting the DČ light measurement resolution. Consequently, the contribution of the secondary Čerenkov background to the charge resolution has the form

$$\Delta Z/Z \propto \frac{\sqrt{Z}}{Z^2} = Z^{-1.5}$$

In this calculation, we have used a conservative  $0.2^\circ$  by 6 ns square integration window for calculating the background contribution. In principle, this can be improved on by matching the detector pixel size and time resolution to the inherent width of the DČ light emission. In our simulation plots, we have used time bins of 500 ps and angular bins of  $0.00375^\circ$ , close to the optimal values.

A third light-related background effect is due to Mie and Rayleigh scattering of Čerenkov light emitted from the EAS electrons. This scattering can deflect light from the EAS Čerenkov component into the DČ light beam. We have undertaken a detailed simulation of the effects of these scattering processes and conclude that Mie scattering will likely affect only the DČ emission from lighter nuclei ( $Z < 6$ ). Heavier nuclei will be unaffected as their DČ light is much stronger than the Mie scattered light from the EAS. For purposes of this paper, the resolution limitations due to atmospheric scattering of the secondary Čerenkov light are included in the secondary Čerenkov background calculation.

### 3.2 Detector Resolution Effects

In addition to the background effects due to light contamination, there will be detector-induced limitations to the charge resolution. These limitations include the core position resolution, angular reconstruction resolution, and the error in the measured signal due to fluctuations in the DČ signal photoelectron statistics (which depends upon the camera quantum efficiency ( $QE$ ) and the mirror or imaging plane area ( $A$ )). In the following calculations we assume  $A = 100$  m<sup>2</sup> and  $QE = 25\%$ .

For typical gamma-ray observatories like VERITAS and HESS, a primary trajectory angular reconstruction error of  $\approx 0.1^\circ$  is expected. In these simulations, we assume the high-resolution cosmic ray detector has a similar angular reconstruction error. The charge resolution error is then computed by comparing average DČ light yields at a mean radius of 80 m for an ensemble of vertical simulated showers with another ensemble of showers with identical charge

and energy, but with a primary zenith angle trajectory of  $0.1^\circ$ . The resulting error is independent of  $Z$ , and very small ( $\Delta Z/Z \approx 0.34\%$ ).

Given a gamma-ray observatory like VERITAS with an array of 10 m diameter primary mirrors, the core position can only be localized to approximately 5 meters. Assuming a 5 meter core resolution error, we examined the change in the DČ light yield as a function of distance from the shower core using the Monte Carlo simulation. Using a linear interpolation of the light yield variation with distance to the shower core, one derives a charge resolution error of 3.1% due to core position uncertainty. This charge resolution error is independent of the primary charge  $Z$ .

Fluctuations in the photon statistics play an important role for low DČ light emission levels (at small  $Z$ ). Since the signal is proportional to  $Z^2$ , the charge resolution scales like

$$\Delta Z/Z \propto \frac{\sqrt{Z^2}}{Z^2} = 1/Z.$$

The magnitude of signal is determined from the Monte Carlo Simulation, assuming the above specified values for QE and  $A$ .

### 3.3 Hadronic Interaction Fluctuations

The primary cosmic ray nuclei will all eventually interact hadronically in the atmosphere. Because of this, the length of the DČ light-emitting region changes from event to event with the fluctuation in the depth of the first interaction. This leads to a subsequent fluctuation in the DČ light yield. Event-to-event fluctuations in the fragmentation process itself yield additional uncertainty.

Studies of these effects with Monte Carlo simulations show that the resulting  $Z$  dependence of the charge resolution is found to be well described by a power law  $\Delta Z/Z \propto Z^{-0.73}$ . An important result is that all possible interaction fluctuations can only result in a *decrease* in the observed DČ light level. For example, although a  $Z = 64$  nucleus might occasionally yield a very low light DČ signal comparable to a  $Z = 26$  or  $Z = 40$  nucleus, a *smaller charge* (e.g.,  $Z = 40$ ) nucleus cannot emit the DČ light intensity of a  $Z = 64$  nucleus. Consequently, interaction fluctuations can only result in an underestimation of the particle charge.

### 3.4 Overall Resolution

The charge resolution expected from the DČ technique is limited by the combination of the various effects described above. In order to be conservative, we have assumed a detection scheme with an imaging plane or mirror area of 100 m<sup>2</sup>, a core location capability of 5 m, a time resolution of 6 ns, and an angular pixel size of  $0.2^\circ$ . Figure 3 shows the charge resolution expected resulting from these effects as a function of charge  $Z$ . For low charges the resolution is dominated by secondary Čerenkov light from the EAS. At higher  $Z$  the core resolution provides the charge resolution limitation. The overall resolution is calculated to be  $\Delta Z/Z \sim 5\%$  for  $Z > 10$ , essentially independent of charge.

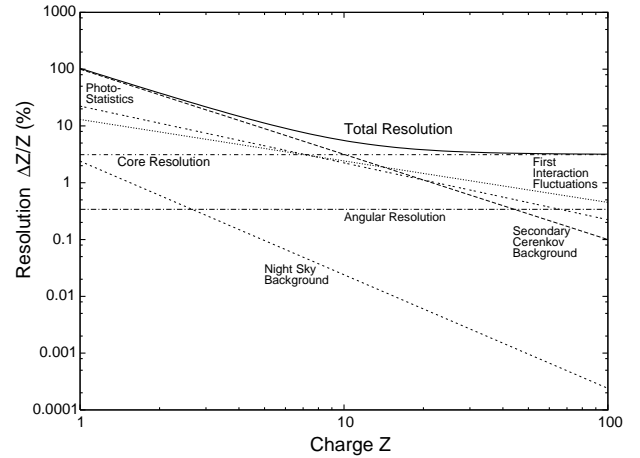


**Fig. 3.** The expected charge resolution  $\Delta Z/Z$  for a detector with an imaging plane area of 100 m<sup>2</sup> and core position resolution 5 m. Horizontal Axis: Primary Charge  $Z$ . Vertical Axis: Charge Resolution  $\Delta Z/Z$  (%).

## 4 Conclusions

We have discussed a new experimental technique which can potentially yield excellent charge resolution measurements ( $\Delta Z/Z < 5\%$  for  $Z = 26$ ) for ground-based observations of high energy cosmic rays. The technique relies upon the observation of the direct Čerenkov light emitted by the primary nucleus before the first nuclear interaction with the Earth's atmosphere. The experimental technique works over an energy range in the TeV-PeV energy range, with the width of the energy window growing like  $Z$  for heavy nuclei.

The average intensity and fluctuations in the DČ light yield have been examined using Monte Carlo simulations. The yield contains the expected  $Z^2$  dependence with fluctuations that are easily understandable in terms of the radial distance of observation, variations in the depth of first hadronic interaction, and the details of the subsequent fragmentation process. Indeed, DČ light measurement appears to provide a method to measure the primary charge independent of any hadronic interaction or fragmentation model.

## References

- D.B. Kieda, S.P. Swordy, and S.P. Wakely, Accepted in Astroparticle Physics (2000). astro-ph/0010554.
- D.B. Kieda, S.P. Swordy, and S.P. Wakely, Proc. 27th ICRC (Hamburg) HE 3.4 (2001).
- K. Sitte, Proc. 9th ICRC (London)(1965) 887.
- M.P. Gough, J. Phys. G: Nucl. Phys. 2 (12) (1976) 965.
- R.K. Sood, Nature 301 (1983) 44.
- J. Clem, *et al.*, Accepted in Astroparticle Physics (2001). astro-ph/0103397.
- A.M. Hillas, J. Phys. G: Nucl. Phys. G8 (1982) 1461.
- A.M. Hillas, J. Phys. G: Nucl. Phys. G8 (1982) 1475.
- D.B. Kieda, Astroparticle Physics 4 (1995) 133.
- D. Heck, *et al.*, Forschungszentrum Karlsruhe Report FZKA 6019 (1998).